Viscous fingering in periodically heterogeneous porous media. I. Formulation and linear instability

A. De Wit
Service de Chimie Physique and Centre for Nonlinear Phenomena and Complex Systems, CP 231 Université Libre de Bruxelles, Campus Plaine, 1050 Brussels, Belgium

G. M. Homsy
Department of Chemical Engineering, Stanford University, Stanford, California 94305-5025

(Received 24 June 1997; accepted 4 September 1997)

We are generally interested in viscously driven instabilities in heterogeneous porous media for a variety of applications, including chromatographic separations and the passage of chemical fronts through porous materials. Heterogeneity produces new physical phenomena associated with the interaction of the flow with the heterogeneity on the one hand, and the coupling between the flow, the concentration of a passive scalar, and the physical properties (here the viscosity) on the other. We pose and solve a model in which the permeability heterogeneity is taken to be periodic in space, thus allowing the interactions of the different physical mechanisms to be carefully studied as functions of the relevant length and time scales of the physical phenomena involved. In this paper, Paper I of a two-part study, we develop the basic equations and the parameters governing the solutions. We then focus on identifying resonant interactions between the heterogeneity and the intrinsic viscous fingering instability. We make analytical progress by limiting our attention to the case of small heterogeneity, in which case the base state flow is only slightly disturbed from a uniform flow, and to linear instability theory, in which the departures from the base state flow are taken to be small. It is found that a variety of resonances are possible. Analytic solutions are developed for short times and for the case of subharmonic resonance between the heterogeneities and the intrinsic instability modes. A parametric study shows this resonance to increase monotonically with the viscosity ratio i.e., with the strength of the intrinsic instability, and to be most pronounced for the case of one-dimensional heterogeneities layered horizontally in the flow direction, as expected on simple physical grounds. When axial variation of the permeability field is also considered, a damping of the magnitude of the response generally occurs, although we find some evidence of local resonances in the case when the axial forcing is commensurate with a characteristic dispersive time. The response exhibits a high frequency roll-off as expected. These concepts of resonant interaction are found to be useful and to carry over to the strongly nonlinear cases treated by numerical methods in Paper II [J. Chem Phys. **107**, 9619 (1997)]. *© 1997 American Institute of Physics.* [S0021-9606(97)50946-9]

I. INTRODUCTION

The problem of viscous instabilities in porous media is one that continues to receive attention in a wide variety of fields due to the ubiquity of applications of flow in porous media. Of particular interest is the occurrence of such instabilities in analytical chemistry applications, notably in both laboratory scale and large scale chromatographic separations in which the property variations of chemical mixtures, in particular, the variation of viscosity with concentration, can drive instabilities and lead to long tails in dispersion and in breakthrough curves. For examples of both experimental and numerical studies of fingering in chromatographic applications, see Refs. 1–5. In addition, there are applications involving the propagation of chemically reacting fronts through porous media,[6] as well as in petroleum recovery and other chemical fixed bed processing.[7]

Our interest and focus in this paper is in viscously driven instabilities in heterogeneous media. By heterogeneous, we mean situations in which variations in the microstructure of the porous media lead to corresponding variations in the flow resistance, as expressed in the permeability. We thus assume a separation of scales in which the spatial variability is negligible over many pore scales—leading to a Darcy level continuum description of the flow—but in which the spatial variability over scales that are large compared to the pore scale cannot be neglected.

There have been significant advances in the understanding of unstable viscous fingering in spatially homogeneous media on the one hand and in the understanding of macrodispersion in heterogeneous media on the other.

In the former case of fingering in homogeneous media, there is an intrinsic scale of fingering set by the speed of the displacement, the viscosity ratio, and the level of dispersion.[8] Direct numerical simulations of nonlinear finger propagation have led to a high level of understanding of the finger interaction mechanisms in both two and three dimensions.[9–12] Dynamical processes such as tip splitting and shielding and their underlying physical mechanisms are now well understood from a conceptual and quantitative perspective.

In the latter case of heterogeneous media, it is necessary to adopt a description of the spatial variability of the permeability field in order to make progress. As will be seen below, the natural quantity arising in the flow equations is the log of the permeability: taking the permeability to be a random stationary function of space with a given variance and correlation statistics has proven a popular model on which to make analytical progress.[13–15] It is now well known that the effect of the heterogeneity over long times and distances can be described in terms of a renormalized permeability, dependent on both the variance and the functional form of the correlations, and an axial dispersion coefficient, which is generally larger than that for homogeneous media.[13–17]

There is ample evidence that permeability heterogeneities interact with viscously driven instabilities in a significant way.[2,18–20] In spite of its importance, relatively little theoretical work has been done on the problem of fingering in the presence of heterogeneities, referred to in the remaining text as ''heterogeneous fingering'' for simplicity. Most if not all of the current understanding of heterogeneous fingering is derived from direct numerical simulations. Tan and Homsy[18] reported a short study of fingering in two-dimensional heterogeneous media which strongly suggested a resonant interaction between the intrinsic scales of fingers and the correlation scale of the permeability field. Tchelepi *et al.*[19] have reported simulations and experiments on stable and unstable displacements which establish the region of parameter space in which heterogeneity will dominate fingering, and vice versa. Similar simulations in other geometries have recently been reported by Sorbie *et al.*[20] It is generally recognized that the nature of heterogeneous fingering depends on the relative importance of the two physical mechanisms leading to flow nonuniformities: instabilities due to an unstable viscosity ratio and preferential flow paths due to the variance of the log permeability. The limiting cases are easy to identify. When the viscosity ratio is large and the variance small, one recovers the limit of finger-dominated dynamics, a well-studied situation. The case of unit viscosity ratio heterogeneous media is also well-studied. A further limiting case is when the permeability contrast overwhelms any effect of viscosity stratification, in which case the flow paths are dictated by the permeability field, and stream tube models may be developed: see, e.g., Ref. 21.

All of these studies help our general understanding of the flow processes in heterogeneous fingering, but have the disadvantage of being difficult to interpret in terms of fundamental mechanisms of interactions between viscous fingering and the underlying nonhomogeneous flow resulting from the permeability variations. This paper and the following one are devoted to developing this understanding through a combination of analytical theory and direct numerical simulation for a particularly simple model of the heterogeneity. The understanding that results sets the stage for further treatment of more complex situations.

Specifically then, we treat viscous fingering in spatially periodic heterogeneous media. As we will see, this allows insight and understanding into the interactions of phenomena on different length scales and a very specific calculation of resonant interactions. Although they have the property of perfect spatial correlation, spatially periodic models of both microstructure and mesoscale variation have been used in the past to similar advantage, and in many cases yield results that are not distinctly different than those for disordered media: see, e.g., Ref. 22 for a discussion of the permeability problem.

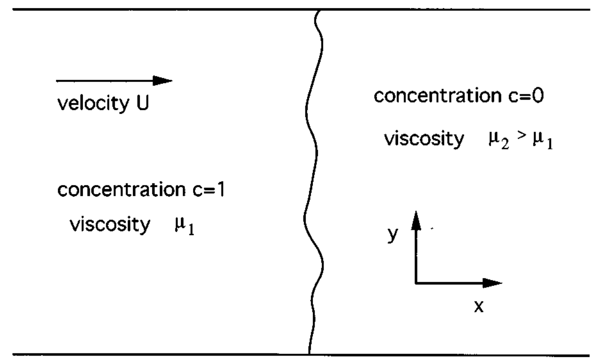

FIG. 1. Sketch of the system.

We present our work in two parts. In this paper (Paper I) the basic equations are established, together with the scaling and description of the spatial variation of permeability. This leads to the identification of the basic dimensionless parameters describing the problem, which are five in number: the amplitude and the two spatial correlation scales of the heterogeneity, the viscosity ratio, and in any bounded geometry, the Peclet number. The paper then focuses on the connection between the ''cellular flow'' that is driven by the permeability variation and the viscous instability that is intrinsic to an unfavorable viscosity ratio. This problem is attacked and solved by a double perturbation expansion in the amplitude of the heterogeneity and the amplitude of the departure from the cellular state. This naturally leads to a discussion of resonances between scales. While the expansion in the amplitude of the heterogeneity is uniform in time, that in the amplitude of disturbances is not. Accordingly, Paper II[23] takes up the issue of direct numerical solutions of the problem, and the interpretation of the results for strongly nonlinear heterogeneous fingering in terms of the analytical understanding gained in part I.

II. BASIC EQUATIONS

We consider a two-dimensional porous medium as depicted in Fig. 1. An incompressible solute with concentration c_1 and viscosity μ_1 is injected from the left boundary with a mean velocity U in the x direction. The porous medium is heterogeneous, i.e., the permeability $\kappa(\mathbf{r})$ is a function of space, and the viscosity is taken to be a given function of the concentration c. The concentration far to the right is taken without loss of generality to be zero, and the viscosity there is μ_2. The dispersion characteristics of the medium are taken to be isotropic, although this assumption can be easily relaxed, and density effects are neglected. The equations of the system are:

$$\nabla \cdot \mathbf{u} = 0, \tag{1}$$

$$\nabla p = -\frac{\mu(c)}{\kappa(\mathbf{r})}\,\mathbf{u}, \tag{2}$$

$$\partial_t c + \mathbf{u}\cdot\nabla c = D\nabla^2 c, \tag{3}$$

where Eqs. (1) and (2) are the continuity equation and Darcy's law while Eq. (3) is the convective-dispersion equation for the concentration c. The viscosity μ of the fluid depends on the concentration through a relation $\mu=\mu(c)$ supposed to be known.

The essential feature of our model is to consider a permeability field varying periodically in both directions of space, i.e., we take

$$F=\ln\left[\frac{\kappa(\mathbf{r})}{\kappa_0}\right]=\sigma\cos qy\cos\alpha x, \tag{4}$$

where κ_0 is the mean permeability and σ is analogous to the square root of the variance in models which take κ to be a stationary random function of space. The parameter σ is thus a measure of the amplitude of the heterogeneities of the porous medium while α and q relate to their correlations lengths along x and y, respectively. We will later take σ to be a small parameter and develop a perturbation scheme for small σ.

The boundary conditions appropriate to spatially infinite systems are a specification of the average pressure gradient (equivalently, a specified, average velocity), periodicity in the direction transverse to the flow, and decay of the concentration to c_1 and zero, respectively, at large distances from the front. Since the fluid is moving with an average mean velocity U, we switch into a moving reference frame taking $x'=x-Ut$ and $\mathbf{u}'=\mathbf{u}-U\mathbf{e}_x$. The evolution equations become:

$$\nabla\cdot\mathbf{u}'=0, \tag{5}$$

$$\nabla p=-\frac{\mu(c)}{\kappa(\mathbf{r}'+U\mathbf{e}_x t)}\,(\mathbf{u}'+U\mathbf{e}_x), \tag{6}$$

$$\partial_t c+\mathbf{u}'\cdot\nabla c=D\nabla^2 c \tag{7}$$

and hence

$$F'=\ln\left[\frac{\kappa(\mathbf{r}'+U\mathbf{e}_x t)}{\kappa_0}\right]=\sigma\cos qy\cos(\alpha x'+\alpha Ut). \tag{8}$$

Using diffusive scales, we introduce the nondimensional variables $\tilde{\mathbf{r}}=\mathbf{r}'U/D$, $\tilde{\mathbf{u}}=\mathbf{u}'/U$, $\tilde{t}=tU^2/D$, $\overline{\mu}=\mu/\mu_1$, $\tilde{p}=p\kappa_0/\mu_1 D$, $\tilde{\kappa}=\kappa/\kappa_0$, $\tilde{c}=c/c_1$, and $\tilde{q}=qD/U$, $\tilde{\alpha}=\alpha D/U$. After dropping the tildes, we arrive at the following nondimensional equations in the moving frame:

$$\nabla\cdot\mathbf{u}=0, \tag{9}$$

$$\nabla p=-\frac{\mu(c)}{\kappa(\mathbf{r}+\mathbf{e}_x t)}\,(\mathbf{u}+\mathbf{e}_x), \tag{10}$$

$$\partial_t c+\mathbf{u}\cdot\nabla c=\nabla^2 c, \tag{11}$$

$$\mu=\mu(c) \tag{12}$$

with

$$F=\ln[\kappa(\mathbf{r}+\mathbf{e}_x t)]$$
$$=\sigma\cos qy[\cos\alpha x\cos\alpha t-\sin\alpha x\sin\alpha t)]. \tag{13}$$

Here q and α are the dimensionless wave numbers of the heterogeneity, and can be thought of as inverse Peclet numbers. We express these equations in terms of the stream function $\psi(x,y)$ such that $u=\partial\psi/\partial y$, $v=-\partial\psi/\partial x$, where u,v are the longitudinal and transverse velocity components, respectively. We finally have our starting equations:

$$\nabla^2\psi=R(c_x\psi_x+c_y\psi_y+c_y)+F_x\psi_x+F_y\psi_y+F_y, \tag{14}$$

$$c_t+c_x\psi_y-c_y\psi_x=\nabla^2 c \tag{15}$$

with $R=-d(\ln\mu)/dc=\ln(M)$, where M is the viscosity ratio, and F is given by Eq. (13). As discussed by Meiburg and Homsy,[24] Eq. (14) shows that the vorticity $w(x,y)=-\nabla^2\psi$ is generated by mobility (concentration) gradients or permeability gradients which are inclined to the local velocity vector. With this interpretation, it becomes obvious that even in the absence of any viscosity stratification, there will be a vortical flow, dependent on the magnitude of σ, that represents a departure from uniform displacement. We will refer to this flow as the ''cellular flow,'' since for our model, it has a period structure that mimics that of the permeability field.

Our purpose is now to first construct a solution for this cellular flow, and then to study its stability. Accordingly, we refer to this flow as the ''stationary state,'' analogous to a ''steady state'' in more conventional stability analyses, and denote the solutions by the subscript s. The cellular flow is a solution of Eqs. (14) and (15), which in the moving frame is driven by a forcing that is time periodic with a frequency related to the transverse wave number. Thus the cellular flow is both time and spatially dependent, and, as we will see, its description is nontrivial. While, in general, it is necessary to solve the coupled set of nonlinear equations (14) and (15), we adopt an approach that is common in the theory of macrodispersion, i.e., we develop the solution as a perturbation expansion in the magnitude of the heterogeneity.[13,14,16,17] While the range of validity of the expansion is, of course, unknown, higher order perturbation theory for the unit mobility ratio case suggests that it is reasonably large.[16] (It is useful to recall that the expansion is in terms of the natural logarithm of the permeability heterogeneity rather than the permeability itself.)

III. PERIODIC STATIONARY STATE

We look for a periodic stationary solution to the system of Eqs. (14) and (15) of the form:

$$\psi_s=\psi_{00}+\sigma\psi_{01}, \tag{16}$$

$$c_s=c_{00}+\sigma c_{01}, \tag{17}$$

where, of course, the leading order terms are just the solutions for a homogeneous permeability field, and are well-known. At order σ^0, the stationary state in the moving frame is

$$\psi_{00}=0, \tag{18}$$

$$c_{00}=\frac{1}{2}\left[1-\mathrm{erf}\left(\frac{x}{2\sqrt{t}}\right)\right]. \tag{19}$$

The stationary state is just the one-dimensional solution for which the velocity is constant and the concentration near the front exhibits dispersive spreading in the axial direction.

At order σ^1, ψ_{01} and c_{01} are solutions of a partial differential equations system with a forcing term due to the spatial dependence of the permeability field which, in the moving frame, gets expressed as both temporal and spatial dependence as follows:

$$(\nabla^2+RG\partial_x)\psi_{01}-R\partial_y c_{01} = F_y=-q\sin qy[\cos\alpha x\cos\alpha t-\sin\alpha x\sin\alpha t], \tag{20}$$

$$G\partial_y\psi_{01}+(\nabla^2-\partial_t)c_{01}=0, \tag{21}$$

where $G=G(x)=-\partial c_{00}/\partial x$ is the gradient of the concentration. In operator notation, we must solve the system

$$L\begin{pmatrix}\psi_{01}\\ c_{01}\end{pmatrix}=\begin{pmatrix}F_y\\ 0\end{pmatrix} \tag{22}$$

with

$$L=\begin{pmatrix}\nabla^2+RG\partial_x & -R\partial_y\\ G\partial_y & \nabla^2-\partial_t\end{pmatrix}. \tag{23}$$

We identify this system as a nonhomogeneous, linear, variable coefficient system, and first focus on the forced solutions. (The eigenfunctions of the operator L will become relevant for the stability problem treated below.) This system admits a solution of the form:

$$\Psi_{01}=\begin{pmatrix}\psi_{01}\\ c_{01}\end{pmatrix}=\begin{pmatrix}\hat{\psi}_{01}(x,t)\sin qy\\ \hat{c}_{01}(x,t)\cos qy\end{pmatrix}. \tag{24}$$

Since the only time dependence comes from the forcing term, we can separate the x and t dependence in $\hat{\psi}_{01}(x,t)$ and $\hat{c}_{01}(x,t)$ by writing

$$\begin{pmatrix}\hat{\psi}_{01}(x,t)\\ \hat{c}_{01}(x,t)\end{pmatrix}=\begin{pmatrix}\psi^c_{01}(x)\cos\alpha t-\psi^s_{01}(x)\sin\alpha t\\ c^c_{01}(x)\cos\alpha t-c^s_{01}(x)\sin\alpha t\end{pmatrix}. \tag{25}$$

The functions $\psi^c_{01}(x)$, $\psi^s_{01}(x)$, $c^c_{01}(x)$, and $c^s_{01}(x)$ are then found as solutions of the following system of equations:

$$(d_x^2-q^2+RGd_x)\psi^c_{01}+qRc^c_{01}=-q\cos\alpha x, \tag{26}$$

$$-(d_x^2-q^2+RGd_x)\psi^s_{01}-qRc^s_{01}=q\sin\alpha x, \tag{27}$$

$$Gq\psi^c_{01}+(d_x^2-q^2)c^c_{01}+\alpha c^s_{01}=0, \tag{28}$$

$$-Gq\psi^s_{01}-(d_x^2-q^2)c^s_{01}+\alpha c^c_{01}=0. \tag{29}$$

In general, it is necessary to employ numerical techniques to solve for the Fourier coefficients ψ^c_{01},ψ^s_{01} and c^c_{01},c^s_{01}, since the coefficients of these equations are x dependent as a result of the front having a structure, expressed through $G(x)$. But as will be seen in later sections, it is possible to make analytical progress at short times, for which $G(x)$ may be approximated as a delta function.

This completes the representation of the stationary state through first order in σ. In principle, the perturbation scheme can be continued, but the technical details and complexity quickly become overwhelming.

IV. LINEAR STABILITY ANALYSIS

We wish to consider the stability of the cellular flow described above and we will exploit the use of perturbation theory in σ, which as we will see, will lead to a perturbed eigenvalue problem. In the usual way, we perturb the base state (ψ_s,c_s) by fluctuations of order ϵ and solve for the dynamics of these fluctuations. Consistent with the representation of the stationary state, we assume a perturbation expansion in σ for both the stationary state and the eigenfunctions of the stability problem as follows:

$$\psi=\psi_s+\epsilon\psi_1=\sigma\psi_{01}+\epsilon\psi_{10}+\epsilon\sigma\psi_{11}, \tag{30}$$

$$c=c_s+\epsilon c_1=c_{00}+\sigma c_{01}+\epsilon c_{10}+\epsilon\sigma c_{11}. \tag{31}$$

We comment here that the entire approach may be compactly developed as a double expansion in the two small parameters σ and ϵ. At order $\epsilon^1\sigma^0$, we recover the problem of viscous fingering in homogeneous media. Of particular interest here are the dynamics at order $\epsilon^1\sigma^1$, which gives the coupling between the viscous fingering instability and the flow driven by permeability heterogeneity. The details are as follows.

A. Order $\epsilon^1\sigma^0$

At this order, the perturbation equations for the fluctuations reduce to

$$L\begin{pmatrix}\psi_{10}\\ c_{10}\end{pmatrix}=0, \tag{32}$$

which are identical to those analyzed in some detail by Tan and Homsy.[8] Normal mode solutions are of the form

$$\Psi_{10}=\begin{pmatrix}\psi_{10}\\ c_{10}\end{pmatrix}=\begin{pmatrix}\hat{\psi}_{10}(x)\sin ky\\ \hat{c}_{10}(x)\cos ky\end{pmatrix}e^{\omega t}. \tag{33}$$

At this order, $\hat{\psi}_{10}(x)$ and $\hat{c}_{10}(x)$ are thus found as eigensolutions of

$$(d_x^2-k^2+RGd_x)\hat{\psi}_{10}+Rk\hat{c}_{10}=0, \tag{34}$$

$$Gk\hat{\psi}_{10}+(d_x^2-k^2-\omega)\hat{c}_{10}=0. \tag{35}$$

Combining these two equations by taking

$$\hat{c}_{10}(x)=-\frac{1}{Rk}[d_x^2-k^2+RG(x)d_x]\hat{\psi}_{10}(x) \tag{36}$$

we may express this as a fourth-order differential equation for $\hat{\psi}_{10}$:

$$(d_x^2-k^2-\omega)(d_x^2-k^2+RGd_x)\hat{\psi}_{10}-RGk^2\hat{\psi}_{10}=0. \tag{37}$$

This equation is an eigenvalue problem with boundary conditions specifying that disturbances decay to zero at $x\to\pm\infty$. For general $G(x)$, this equation can be solved numerically to find the eigenvalue ω and the dispersion relation.[8] The corresponding eigenfunctions $\hat{\psi}_{10}(x)$ and $\hat{c}_{10}(x)$ can also be computed.

The general properties of the dispersion relation will be of importance in the next section. It is generally found that the growth rate is zero for long waves, $k=0$, becomes positive for unstable viscosity ratios as k increases, and then

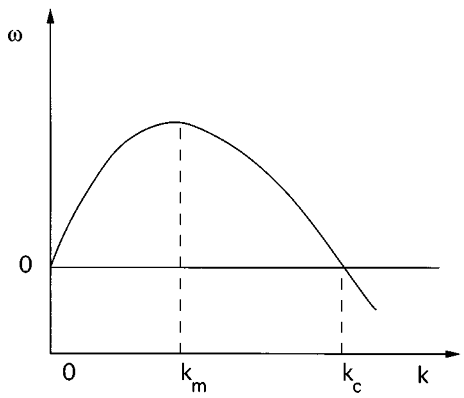

FIG. 2. Sketch of the typical dispersion relation of the viscous fingering instability in a homogeneous porous medium. The growth rate ω of the instability is positive for a band of wave numbers k between 0 and the cutoff wave number k_c. The maximum growth rate occurs for wave number k_m.

exhibits a cutoff wave number above which all fluctuations are damped. These properties may be established analytically for short times, and are robust features of the dispersion relation at later times. A detailed discussion is given in Ref. 8. A typical dispersion relation is given in Fig. 2. We denote the wave number corresponding to the maximum growth rate at any time as k_m.

B. Order $\epsilon^1\sigma^1$

We now consider the dynamics of fluctuations induced by the unstable viscosity ratio and potentially influenced by coupling with the cellular component of the stationary state. The evolution equations at order $\epsilon^1\sigma^1$ are:

$$(\nabla^2+RG\partial_x)\psi_{11}-R\partial_y c_{11} =R[c_{01x}\psi_{10x}+c_{01y}\psi_{10y}+c_{10x}\psi_{01x}+c_{10y}\psi_{01y}] +F_x\psi_{10x}+F_y\psi_{10y}=I_1, \quad (38)$$

$$G\partial_y\psi_{11}+(\nabla^2-\partial_t)c_{11}=c_{10x}\psi_{01y}+c_{01x}\psi_{10y}-c_{10y}\psi_{01x} -c_{01y}\psi_{10x}=I_2, \quad (39)$$

which can be written in short as

$$L\begin{pmatrix}\psi_{11}\\ c_{11}\end{pmatrix}=\begin{pmatrix}I_1\\ I_2\end{pmatrix} \quad (40)$$

or also $L\Psi_{11}=I$. Let us obtain an explicit form for I_1 and I_2. Replacing ψ_{10},c_{10} by Eq. (33) and taking ψ_{01} and c_{01} as Eq. (24) we get after collecting terms:

$$I_1=[A(x)\cos\,\alpha t+B(x)\sin\,\alpha t]\sin(q-k)ye^{\omega t} +[C(x)\cos\,\alpha t+D(x)\sin\,\alpha t]\sin(q+k)ye^{\omega t}, \quad (41)$$

$$I_2=[E(x)\cos\,\alpha t+H(x)\sin\,\alpha t]\cos(q-k)ye^{\omega t} +[J(x)\cos\,\alpha t+K(x)\sin\,\alpha t]\cos(q+k)ye^{\omega t}, \quad (42)$$

where A,B,C,D,E,H,J,K are given in Appendix A.

Equation (40) is at the heart of our analysis, as it shows how the eigenmodes of the instability, characterized by wave number k, interact with the spatial variation of the cellular flow, characterized by wave number q, to give a forcing for the evolution of fluctuations of wave number $k\pm q=k_m$ at order $\epsilon^1\sigma^1$. Solutions of this equation will involve the eigenmodes of the homogeneous problem, i.e., the eigenmodes of the operator L, but they add little to the dynamics and can be easily absorbed into the solutions at $\epsilon^1\sigma^0$. The case of interest is when the nonhomogeneous terms on the right-hand side of Eq. (40) force the growth of the mode of maximum growth rate through resonant interactions. Forcings of modes of wave numbers different than k_m are not expected to compete in any significant fashion with the intrinsic growth of the most unstable wave, since this forced growth will be slower than the most unstable wave. Thus, as is well-known, and is evident from Eqs. (41) to (42), the important resonant interaction occurs when $k\pm q=k_m$. We distinguish two cases, that of subharmonic resonance and that of a sideband resonance.

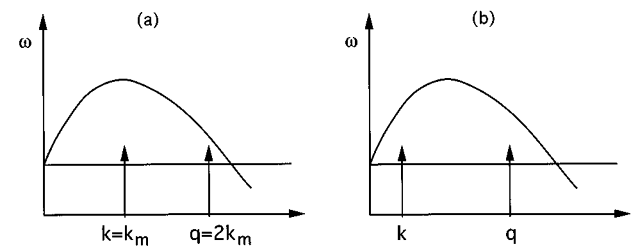

FIG. 3. Sketch of the possible resonances between one unstable wave number k of the viscous instability and the wave number q of the permeability heterogeneities. (a) Subharmonic resonance when $q=2k_m$ and $k=k_m$ such that $(q-k)=k_m$. (b) Sideband resonance between arbitrary k and q such that $(q-k)=k_m$.

Case A. Subharmonic resonance. In this case, the choice $q=2k_m$ leads to forcing of the fastest growing mode with $q-k=(2k_m-k_m)=k_m$, as well as (unimportant) forcing of a strongly damped third harmonic. Figure 3(a) illustrates the situation in a schematic fashion.

Case B. Sideband resonance. This case recognizes the fact that we expect both q and k to have a finite bandwidth and will not, in general, by characterized by pure modes. The instability wave number k has a spectrum because we expect fluctuations of all scales to be present in any physical experiment. The parameter q also has a spectrum in the case of disordered media, and is a free parameter in our spatially periodic model. Thus we have the possibility of resonances between the sidebands $q\pm k=k_m$ for a range of q and k. The case $q-k=k_m$ is shown schematically in Fig. 3(b) the case $q+k=k_m$ is directly analogous.

V. SOLUTION STRUCTURE OF THE $O(\epsilon\sigma)$ EQUATIONS

We now discuss the solution technique used to solve the partial differential equations (38) and (39). We do this by reducing them to ordinary differential equations by projecting them onto the eigenmodes of the operator L using Galerkin methods. Under the conditions of resonance, we seek a solution of the form

$$\Psi_{11}=\begin{pmatrix}\psi_{11}\\ c_{11}\end{pmatrix}=\begin{pmatrix}\mathscr{X}(t)\hat{\psi}_{10}(x)\sin k_m y\\ \mathscr{Y}(t)\hat{c}_{10}(x)\cos k_m y\end{pmatrix}, \quad (43)$$

where k_m is an unstable wave number of the linear stability analysis, $\hat{\psi}_{10}(x),\hat{c}_{10}(x)$ are the eigenmodes, and $\mathscr{X},\mathscr{Y}$ are amplitude functions to be determined. Inserting Eq. (43) into Eq. (40) and projecting the first and second of these equations, respectively, on $\hat{\psi}_{10}(x)$ and $\hat{c}_{10}(x)$, we get the following system of ordinary differential equations

$$a_{11}\mathscr{X}(t)+a_{12}\mathscr{Y}(t)=e^{\omega t}[b_{11}\cos\alpha t+b_{12}\sin\alpha t], \quad (44)$$

$$a_{21}\mathscr{X}(t)+a_{22}\mathscr{Y}(t)-n\dot{\mathscr{Y}}(t)=e^{\omega t}[b_{21}\cos\alpha t+b_{22}\sin\alpha t], \quad (45)$$

where the coefficients n, a_{ij}, and b_{ij} are detailed in Appendix B and the dot stands for a time derivative. Since Eq. (44) is algebraic, $\mathscr{X}$ can be eliminated from these equations by taking

$$\mathscr{X}(t)=-\frac{a_{12}}{a_{11}}\mathscr{Y}(t)+\frac{e^{\omega t}}{a_{11}}[b_{11}\cos\alpha t+b_{12}\sin\alpha t], \quad (46)$$

to arrive at the following amplitude equation for $\mathscr{Y}$:

$$\dot{\mathscr{Y}}(t)-\lambda\mathscr{Y}(t)=e^{\omega t}[\mathscr{C}\cos\alpha t+\mathscr{S}\sin\alpha t], \quad (47)$$

with

$$\lambda=\frac{1}{n}\left[a_{22}-\frac{a_{21}a_{12}}{a_{11}}\right], \quad (48)$$

$$\mathscr{C}=\frac{1}{n}\left[\frac{b_{11}a_{21}}{a_{11}}-b_{21}\right], \quad (49)$$

$$\mathscr{S}=\frac{1}{n}\left[\frac{a_{21}b_{12}}{a_{11}}-b_{22}\right]. \quad (50)$$

The solution of Eq. (47) is

$$\mathscr{Y}(t)=e^{\omega t}[\gamma\cos\alpha t+\xi\sin\alpha t] \quad (51)$$

with

$$\gamma=\frac{\mathscr{C}(\omega-\lambda)-\mathscr{S}\alpha}{(\omega-\lambda)^2+\alpha^2}, \quad (52)$$

$$\xi=\frac{\mathscr{S}(\omega-\lambda)+\mathscr{C}\alpha}{(\omega-\lambda)^2+\alpha^2}. \quad (53)$$

The interpretation of the resulting solution is suggested by the analysis of simple model equations, from which it is possible to establish Eq. (51) as the first term of the expansion of an exponential. Accordingly, combining expressions (33), (43), and (51), we have at order ϵ:

$$c_{10}+\sigma c_{11}=\hat{c}_{10}(x)\cos(k_m y)e^{\omega t}[1+\sigma(\gamma\cos\alpha t+\xi\sin\alpha t)] \quad (54)$$

$$=\hat{c}_{10}(x)\cos(k_m y)e^{\omega t+\sigma(\gamma\cos\alpha t+\xi\sin\alpha t)}. \quad (55)$$

Since the temporal phase of the permeability field is arbitrary, Eq. (55) is equivalent to

$$c_1\sim e^{(\omega+\sigma\omega_1)t}, \quad (56)$$

where

$$\omega_1=\sqrt{\gamma^2+\xi^2} \quad (57)$$

is the root mean square amplitude of the $O(\sigma)$ oscillatory terms in Eq. (55). The magnitude of ω_1 shows then how much the heterogeneities of the porous medium enhance the growth rate of the viscous fingers.

VI. CALCULATIONS FOR $G=\delta(x)$

We have developed the approach and the equations necessary to compute the correction to the growth rate of a viscous fingering instability due to permeability heterogeneities. At times $t>0$, the base state is spatially dependent and the eigensolutions Ψ_{01} and the cellular flow Ψ_{10} must be computed numerically, which, in principle, can be done. However, in order to gain insight into the results of the theory, it is advantageous to obtain analytical results. We do so in this section, in which we solve the problem for short times, for which the gradient $G=\delta(x)$.

A. Stationary state

At order $\epsilon^0\sigma^1$, we are looking for a solution of the form:

$$\Psi_{01}=\begin{pmatrix}\psi_{01}\\ c_{01}\end{pmatrix}=\begin{pmatrix}[\psi_{01}^c(x)\cos\alpha t-\psi_{01}^s(x)\sin\alpha t]\sin qy\\ [c_{01}^c(x)\cos\alpha t-c_{01}^s(x)\sin\alpha t]\cos qy\end{pmatrix}, \quad (58)$$

where $\psi_{01}^c(x)$, $\psi_{01}^s(x)$, $c_{01}^c(x)$, and $c_{01}^s(x)$ obey the following system of equations:

$$(d_x^2-q^2+RGd_x)\psi_{01}^c+qRc_{01}^c=-q\cos\alpha x, \quad (59)$$

$$-(d_x^2-q^2+RGd_x)\psi_{01}^s-qRc_{01}^s=q\sin\alpha x, \quad (60)$$

$$Gq\psi_{01}^c+(d_x^2-q^2)c_{01}^c+\alpha c_{01}^s=0, \quad (61)$$

$$-Gq\psi_{01}^s-(d_x^2-q^2)c_{01}^c+\alpha c_{01}^c=0, \quad (62)$$

with $G=\delta(x)$. Let us first consider Eqs. (61) and (62). The solutions to the right of the front $c_r^{c,s}(x>0)$ and to the left $c_l^{c,s}(x<0)$ where $G(x)=0$ obey the homogeneous equations:

$$(d_x^2-q^2)c_{r,l}^c+\alpha c_{r,l}^s=0, \quad (63)$$

$$-(d_x^2-q^2)c_{r,l}^s+\alpha c_{r,l}^c=0. \quad (64)$$

Applying decay conditions at infinity, the solutions are

$$c_r^c=[A_r^c\cos(\beta x)+B_r^c\sin(\beta x)]\exp(-\rho x), \quad x>0, \quad (65)$$

$$c_l^c=[A_l^c\cos(\beta x)+B_l^c\sin(\beta x)]\exp(\rho x), \quad x<0, \quad (66)$$

$$c_r^s=[A_r^s\cos(\beta x)+B_r^s\sin(\beta x)]\exp(-\rho x), \quad x>0, \quad (67)$$

$$c_l^s=[A_l^s\cos(\beta x)+B_l^s\sin(\beta x)]\exp(\rho x), \quad x<0, \quad (68)$$

where

$$\rho=\sqrt{\frac{q^2+\sqrt{q^4+\alpha^2}}{2}}, \quad (69)$$

$$\beta=\frac{\alpha}{\sqrt{2(q^2+\sqrt{q^4+\alpha^2})}}. \quad (70)$$

The continuity of c_{01}^s and c_{01}^c at $x=0$ imposes $A_r^c=A_l^c$, $A_r^s=A_l^s$. Moreover, inserting solutions (65)–(68) into (63) or (64) we have

$$A_{r,l}^s=B_{r,l}^c=C_1, \quad (71)$$

$$-A_{r,l}^c=B_{r,l}^s=C_2. \quad (72)$$

This leads to expressions for c_l^c, c_l^s, c_r^c, and c_r^s that depend only on two remaining unknowns C_1 and C_2:

$$c_r^c=[-C_2\cos(\beta x)+C_1\sin(\beta x)]\exp(-\rho x), \quad (73)$$

$$c_l^c=[-C_2\cos(\beta x)+C_1\sin(\beta x)]\exp(\rho x), \quad (74)$$

$$c_r^s=[C_1\cos(\beta x)+C_2\sin(\beta x)]\exp(-\rho x), \quad (75)$$

$$c_l^s=[C_1\cos(\beta x)+C_2\sin(\beta x)]\exp(\rho x). \quad (76)$$

We now consider Eqs. (59) and (60), focusing on the domain $(x\neq 0)$ where the solutions are $\psi_r^{c,s}$ on the right $(x>0)$ and $\psi_l^{c,s}$ on the left $(x<0)$. These equations are simplified if combined with Eqs. (63) and (64):

$$(d_x^2-q^2)\left(\psi_{r,l}^c+\frac{qR}{\alpha}c_{r,l}^s\right)=-q\cos\alpha x, \quad (77)$$

$$(d_x^2-q^2)\left(\psi_{r,l}^s-\frac{qR}{\alpha}c_{r,l}^c\right)=-q\sin\alpha x. \quad (78)$$

Again applying decay conditions at infinity and continuity at $x=0$, the solutions of these equations read:

$$\psi_r^c=C_3\exp(-qx)-\frac{qR}{\alpha}c_r^s+\frac{q}{q^2+\alpha^2}\cos(\alpha x), \quad (79)$$

$$\psi_l^c=C_3\exp(qx)-\frac{qR}{\alpha}c_l^s+\frac{q}{q^2+\alpha^2}\cos(\alpha x), \quad (80)$$

$$\psi_r^s=C_4\exp(-qx)+\frac{qR}{\alpha}c_r^c+\frac{q}{q^2+\alpha^2}\sin(\alpha x), \quad (81)$$

$$\psi_l^s=C_4\exp(qx)+\frac{qR}{\alpha}c_l^c+\frac{q}{q^2+\alpha^2}\sin(\alpha x). \quad (82)$$

We comment in passing that the terms proportional to $q/(q^2+\alpha^2)$ represent the persistent cellular flow driven in the bulk of the fluid by the interaction of the base flow with the permeability field flow alone, while the other terms represent homogeneous solutions that decay away from the front, and which are required to fully satisfy the homogeneous coupled equations. Furthermore, integrating Eqs. (59)–(62) from 0^- to 0^+ imposes the following constraints:

$$d_x\psi_r^c(0)-d_x\psi_l^c(0)+\frac{R}{2}[d_x\psi_r^c(0)+d_x\psi_l^c(0)]=0, \quad (83)$$

$$d_x\psi_r^s(0)-d_x\psi_l^s(0)+\frac{R}{2}[d_x\psi_r^s(0)+d_x\psi_l^s(0)]=0, \quad (84)$$

$$q\psi_r^c(0)+d_xc_r^c(0)-d_xc_l^c(0)=0, \quad (85)$$

$$q\psi_r^s(0)+d_xc_r^s(0)-d_xc_l^s(0)=0. \quad (86)$$

Inserting solutions (73)–(76) and (79)–(82) inside these conditions allows the determination of the constants C_1, C_2, C_3, and C_4:

$$C_1=\frac{qR\alpha}{D}(-qR^2\alpha\beta+4q^3-4\rho q^2+4\alpha^2\rho), \quad (87)$$

$$C_2=-\frac{\alpha q^2}{D}[2R^2(\rho\alpha-q\alpha-\beta q)+8\rho\alpha], \quad (88)$$

$$C_3=\frac{R^2q}{D}[-q^2R^2\beta(\alpha+\beta)+4\rho(q^3-\rho q^2+\alpha^2\rho+\beta\alpha q)], \quad (89)$$

$$C_4=-\frac{R}{D}[2R^2q(\rho\alpha q^2+\beta\rho\alpha^2-q^3\beta-q^3\alpha)+8\rho^2\alpha(q^2-\alpha^2)], \quad (90)$$

with

$$D=(q^2+\alpha^2)[qR^2(q\beta^2R^2+4q^3-8\rho q^2+4q\rho^2-8\beta\rho\alpha)+16\rho^2\alpha^2]. \quad (91)$$

As a conclusion, the presence of the permeability field introduces σ-order corrections to the concentration and the stream function that are given by Eqs. (73)–(76) and (79)–(82).

B. Growth rate in homogeneous systems

The growth rate of the viscous fingering instability in a homogeneous system is computed analytically at order $\epsilon^1\sigma^0$ by doing a linear stability analysis along the one performed by Tan and Homsy[8] when $G=\delta(x)$. Here, we summarize their findings. If $G=\delta(x)$ and assuming decaying conditions at $x\to\pm\infty$, the fourth-order differential equation (37) for $\hat{\psi}_{10}$ admits the following solution:

$$\hat{\psi}_{10}(x)=A_1e^{lx}+B_1e^{kx}, \quad x<0, \quad (92)$$

$$\hat{\psi}_{10}(x)=A_2e^{-lx}+B_2e^{-kx}, \quad x>0, \quad (93)$$

where $l^2=k^2+\omega$. Imposing continuity of the velocity, of the gradient of pressure, and of the concentration at $x=0$, we obtain the dispersion relation:

$$\omega=[Rk-k^2-k\sqrt{k^2+2Rk}]/2. \quad (94)$$

The most dangerous mode corresponds to $k_m=0.118R$ and $\omega_m=0.0225R^2$. We can compute the constants $A_1=A_2=-kA/l$ and $B_1=B_2=A$. Since these are eigenfunctions, A is arbitrary, so we conveniently put it equal to 1 and have thus

$$\hat{\psi}_{10}(x)=\frac{-k}{l}e^{lx}+e^{kx}, \quad x<0,$$

$$\hat{\psi}_{10}(x)=\frac{-k}{l}e^{-lx}+e^{-kx}, \quad x<0. \quad (95)$$

It is straightforward to see that the derivative of $\hat{\psi}_{10}$ is equal to zero at $x=0$. Hence the term $RG(x)d\hat{\psi}_{10}/dx$ in Eq. (36) vanishes for any value of x if $G(x)=\delta(x)$ and we have

$$\hat{c}_{10}(x)=\frac{1}{Rl}(l^2-k^2)e^{lx}, \quad x<0,$$
$$\hat{c}_{10}(x)=\frac{1}{Rl}(l^2-k^2)e^{-lx}, \quad x>0. \tag{96}$$

C. Correction to the growth rate due to the heterogeneities

We have shown previously that the correction ω_1 to the growth rate ω in heterogeneous systems takes the form

$$\omega_1=\sqrt{\gamma^2+\xi^2}, \tag{97}$$

where γ and ζ are functions of the integrals a_{ij} and b_{ij} given in Appendix B through the relations (48)–(50) and (52)–(53). Using $\hat{\psi}_{10}(x)$ given by Eq. (95) and $\hat{c}_{10}(x)$ given by Eq. (96), we have

$$a_{11}=-\frac{k(k+2l)(l-k)^2}{l^3}=-a_{12}, \tag{98}$$

$$a_{21}=\frac{k(l^2-k^2)(l-k)}{Rl^2}, \tag{99}$$

$$a_{22}=\frac{(l-k)^3(k+l)^3}{R^2l^3}, \tag{100}$$

$$n=\frac{(l^2-k^2)^2}{R^2l^3}. \tag{101}$$

It is straightforward to evaluate these formulas for specific values of the parameters. For example, using the results that $k=k_m=0.118R$, $\omega=\omega_m=0.0225R^2$, we have for $R=3$, $a_{11}=-0.135\,05=-a_{12}$, $a_{21}=0.015\,93$, $a_{22}=0.004\,92$, and $n=0.024\,28$.

Among the possible resonances discussed above, we focus here on the subharmonic resonances that come into play when $q=2k_m$, $k=k_m$ such that $(q-k)=k_m$. Using the MAPLE symbolic calculator program, we compute the integrals

$$b_{11}=\int_{-\infty}^{+\infty}\hat{\psi}_{10}(x)A(x)dx, \tag{102}$$

$$b_{12}=\int_{-\infty}^{+\infty}\hat{\psi}_{10}(x)B(x)dx, \tag{103}$$

$$b_{21}=\int_{-\infty}^{+\infty}\hat{c}_{10}(x)E(x)dx, \tag{104}$$

$$b_{22}=\int_{-\infty}^{+\infty}\hat{c}_{10}(x)H(x)dx, \tag{105}$$

where A, B, E, and H are given in Appendix A. The correction to the growth rate ω_1 is then straightforwardly computed using expression (57).

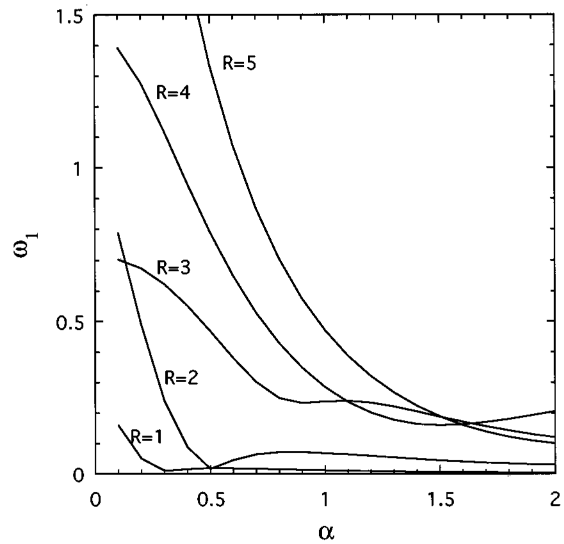

FIG. 4. ω_1 vs α for different values of R. For each value of R, ω_1 is maximum for α close to zero corresponding to layered systems. At low values of R, ω_1 decreases then increases again up to a local maximum characteristic of a resonance with diffusive scales. At higher values of R, ω_1 decays monotonically over the range of α studied.

We have carried out a full parametric study of the dependence of ω_1 on the parameters R and α. These results are shown in Fig. 4 over a range of R and α. Our interpretation of the results is as follows. The general trend of the results is that the correction to the growth rate is the largest for small α, which corresponds to slow periodic variation in the flow direction. Of course, the limit $\alpha=0$ is that of a layered system, in which case the growth of the instability will be significantly enhanced by the ability of the fluid to channel into the more permeable layers. Similar considerations are likely to apply to the case of sideband resonance, but we do not pursue the numerical calculations here. The decay of the response for large α can be explained by recalling that this quantity can be interpreted as either the dimensionless temporal frequency (in the moving frame) at which the front encounters the permeability field, or as a suitably defined inverse Peclet number in which the axial wave number of the permeability field is used to define the characteristic length. In the first interpretation, the high frequency roll-off exhibited for large α is due to the inability of the instability to respond to frequencies much larger than the characteristic diffusion time. In the second interpretation, large α corresponds to a very low Peclet number, indicating the dominance of diffusion in damping any response driven by the periodic forcing.

Figure 4 also indicates that over a limited range of R between 2.0 and 4.0, there is a local maximum in the response at finite α, while the response appears to be monotonic for $R>4$. Figure 5 shows this effect in more detail by focusing on the range $2<R<4$ on an expanded scale for ω_1. Our interpretation of this local maximum is analogous to oscillatory forcing of an unstable system with damping in which the cellular flow provides the periodic forcing. We

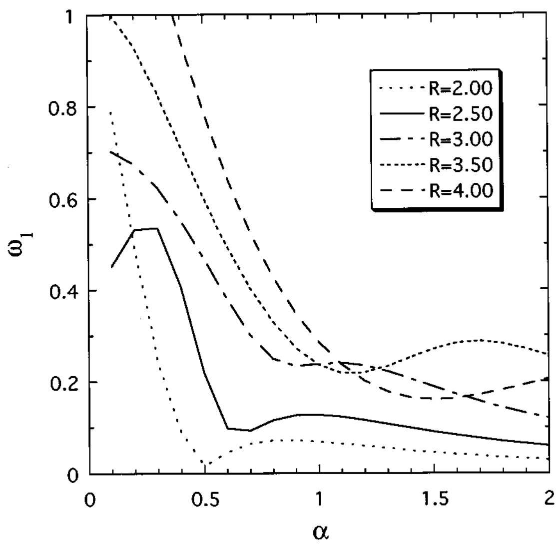

FIG. 5. ω_1 vs α for intermediate values of R. The local maximum is shifted to higher α when R is increasing. This local resonance reaches its maximum for $R=2.5$, $\alpha=0.3$.

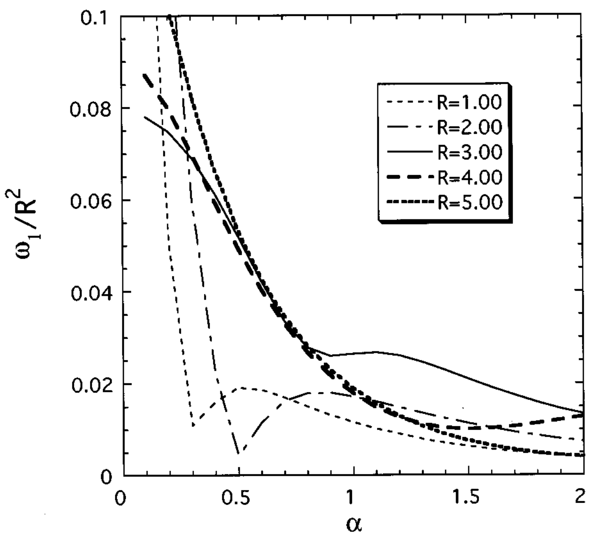

FIG. 6. The scaled growth rate ω_1/R^2 vs α for different values of R.

find that the position of the local maximum, when it occurs, bears an approximate relationship to the wave number of maximum growth rate, k_m as $\alpha=3.3k_m$. From this approximate formula, it is clear that the local maximum occurs when the time scale of the periodic forcing is commensurate with the characteristic diffusive time D/U^2.

We next turn to a discussion of the dependence of ω_1 on R. As noted above, the intrinsic growth rate in homogeneous systems is given by $\omega=\omega_m=0.0225R^2$, indicating, as is well-known, that the instability becomes stronger as the mobility ratio increases. It is therefore appropriate, in comparing the $O(\sigma)$ correction to ω to scale ω_1 by R^2. This is done in Fig. 6, in which the results of Fig. 4 are replotted as ω_1/R^2 vs α. As can be seen, aside from the structure associated with the local resonances, ω_1 scales as R^2 in a fashion similar to that for the homogeneous case. This is particularly true for $R>2$, for which there is a strong suggestion of universality in the normalized results.

Figure 7 summarizes all our results in a contour plot of the normalized response ω_1/R^2 vs R and α. All the features, including the maximum response for small α, the local resonant response for intermediate R, the very flat plateau near $R=3$, and the high frequency roll-off, are made evident by the contour plot.

VII. CONCLUSIONS

Using a model system of heterogeneous porous medium for which the permeability is a periodic function of space we have obtained analytically the correction ω_1 to the homogeneous growth rate of viscous fingers due to the heterogeneities of the medium. This correction occurs because of a subharmonic or a sideband resonance between the wave number of the viscous fingers and the transverse wave number of the permeability field. In the case of the subharmonic resonance we have obtained the correction ω_1 as a function of the mobility ratio and the axial wave number of the permeability. This correction is maximum in the case of layered systems and is an increasing function of the mobility ratio. It features also a local maximum when the frequency of encountering the axial variations of the permeability is commensurate with a characteristic dispersive time. Despite its simplicity the case of periodic porous medium has thus allowed one of the first analytical descriptions of the influence of heterogeneities on the characteristics of the viscous fingering instability. Interesting physical insights into the mechanisms of resonances between the length scales of the

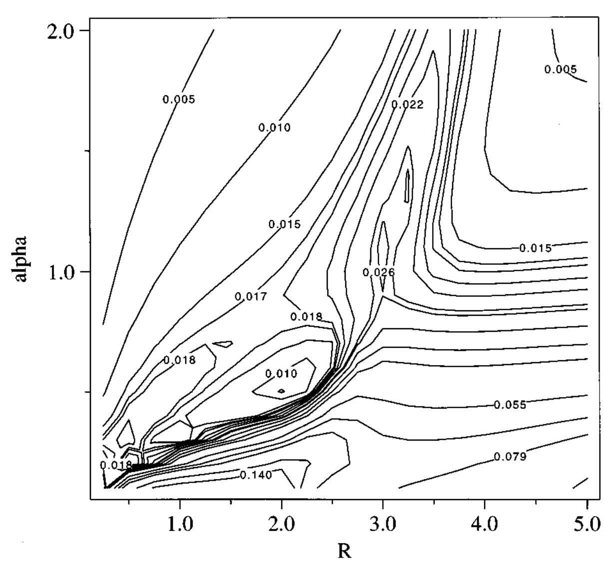

FIG. 7. Contour plot of the normalized correction to the growth rate ω_1/R^2 for different values of R and α. The correction is maximum for R between 0.5 and 2.5 and small α's. Near $R=2$, ω_1/R^2 is decreasing down to a sharp minimum for $\alpha=0.5$. When $R=3$, a large plateau exists for higher values of α such that for $\alpha=1.5$ for instance, the correction will be maximum for $R=3$.

viscous fingers and those of the heterogeneities are hence obtained. These results provide a guideline for the understanding of more realistic but also more complicated permeability fields.

ACKNOWLEDGMENTS

A.D. thanks Daniele Carati for fruitful discussions and the F.N.R.S. (Belgium) and the Petroleum Research Fund through Grant No. PRF-28774-AC9 for financial support. G.M.H. acknowledges support from the U.S. Department of Energy, Office of Basic Energy Sciences.

APPENDIX A

$$2A(x) = -R(\hat{\psi}_{10x} c^c_{01x} - \hat{c}_{10x} \psi^c_{01x}) + Rqk(\hat{c}_{10} \psi^c_{01} - \hat{\psi}_{10} c^c_{01}) + \alpha \hat{\psi}_{10x} \sin \alpha x - kq \hat{\psi}_{10} \cos \alpha x, \tag{A1}$$

$$2B(x) = R(\hat{\psi}_{10x} c^s_{01x} - \hat{c}_{10x} \psi^s_{01x}) - Rqk(\hat{c}_{10} \psi^s_{01} - \hat{\psi}_{10} c^s_{01}) + \alpha \hat{\psi}_{10x} \cos \alpha x + kq \hat{\psi}_{10} \sin \alpha x, \tag{A2}$$

$$2C(x) = R(\hat{\psi}_{10x} c^c_{01x} + \hat{c}_{10x} \psi^c_{01x}) - Rqk(\hat{c}_{10} \psi^c_{01} + \hat{\psi}_{10} c^c_{01}) - \alpha \hat{\psi}_{10x} \sin \alpha x - kq \hat{\psi}_{10} \cos \alpha x, \tag{A3}$$

$$2D(x) = -R(\hat{\psi}_{10x} c^s_{01x} + \hat{c}_{10x} \psi^s_{01x}) + Rqk(\hat{c}_{10} \psi^s_{01} + \hat{\psi}_{10} c^s_{01}) - \alpha \hat{\psi}_{10x} \cos \alpha x + kq \hat{\psi}_{10} \sin \alpha x, \tag{A4}$$

$$2E(x) = q \hat{c}_{10x} \psi^c_{01} + k \hat{\psi}_{10} c^c_{01x} + q \hat{\psi}_{10x} c^c_{01} + k \hat{c}_{10} \psi^c_{01x}, \tag{A5}$$

$$2H(x) = -q \hat{c}_{10x} \psi^s_{01} - k \hat{\psi}_{10} c^s_{01x} - q \hat{\psi}_{10x} c^s_{01} - k \hat{c}_{10} \psi^s_{01x}, \tag{A6}$$

$$2J(x) = q \hat{c}_{10x} \psi^c_{01} + k \hat{\psi}_{10} c^c_{01x} - q \hat{\psi}_{10x} c^c_{01} - k \hat{c}_{10} \psi^c_{01x}, \tag{A7}$$

$$2K(x) = -q \hat{c}_{10x} \psi^s_{01} - k \hat{\psi}_{10} c^s_{01x} + q \hat{\psi}_{10x} c^s_{01} + k \hat{c}_{10} \psi^s_{01x}. \tag{A8}$$

APPENDIX B: COEFFICIENTS OF THE ORDINARY DIFFERENTIAL EQVATIONS

$$a_{11} = \int_{-\infty}^{+\infty} \hat{\psi}_{10}(x) [d_x^2 - k_m^2 + RG(x) d_x] \hat{\psi}_{10}(x) dx, \tag{B1}$$

$$a_{12} = Rk_m \int_{-\infty}^{+\infty} \hat{\psi}_{10}(x) \hat{c}_{10}(x) dx = -a_{11}, \tag{B2}$$

$$a_{21} = k_m \int_{-\infty}^{+\infty} G(x) \hat{\psi}_{10}(x) \hat{c}_{10}(x) dx, \tag{B3}$$

$$a_{22} = \int_{-\infty}^{+\infty} \hat{c}_{10}(x) [d_x^2 - k_m^2] \hat{c}_{10}(x) dx, \tag{B4}$$

$$n = \int_{-\infty}^{+\infty} \hat{c}_{10}(x) \hat{c}_{10}(x) dx. \tag{B5}$$

If we are considering the case $(q-k) = k_m$, then

$$b_{11} = \int_{-\infty}^{+\infty} \hat{\psi}_{10}(x) A(x) dx, \tag{B6}$$

$$b_{12} = \int_{-\infty}^{+\infty} \hat{\psi}_{10}(x) B(x) dx, \tag{B7}$$

$$b_{21} = \int_{-\infty}^{+\infty} \hat{c}_{10}(x) E(x) dx, \tag{B8}$$

$$b_{22} = \int_{-\infty}^{+\infty} \hat{c}_{10}(x) H(x) dx. \tag{B9}$$

For the case $(q+k) = k_m$ then

$$b_{11} = \int_{-\infty}^{+\infty} \hat{\psi}_{10}(x) C(x) dx, \tag{B10}$$

$$b_{12} = \int_{-\infty}^{+\infty} \hat{\psi}_{10}(x) D(x) dx, \tag{B11}$$

$$b_{21} = \int_{-\infty}^{+\infty} \hat{c}_{10}(x) J(x) dx, \tag{B12}$$

$$b_{22} = \int_{-\infty}^{+\infty} \hat{c}_{10}(x) K(x) dx. \tag{B13}$$

[1] M. L. Dickson, T. T. Norton, and E. J. Fernandez, AIChE. J. **43**, 409 (1997).
[2] T. T. Norton and E. J. Fernandez, Ind. Eng. Chem. Res. **35**, 2460 (1996).
[3] M. Czok, A. M. Katti, and G. Guiochon, J. Chromatography **550**, 705 (1991).
[4] E. J. Fernandez, T. T. Norton, W.C. Jung, and J. G. Tsavalas, Biotechnol. Prog. **12**, 480 (1996).
[5] E. Fernandez, C. A. Grotegut, G. W. Braun, K. J. Kirschner, J. R. Staudeher, M. L. Disckson, and V. L. Fernandez, Phys. Fluids **7**, 468 (1995).
[6] D. A. Vasquez, J. W. Wilder, and B. F. Edwards, J. Chem. Phys. **104**, 9926 (1996).
[7] G. M. Homsy, Annu. Rev. Fluid Mech. **19**, 271 (1987).
[8] C. T. Tan and G. M. Homsy, Phys. Fluids **29**, 3549 (1986).
[9] C. T. Tan and G. M. Homsy, Phys. Fluids **31**, 1330 (1988).
[10] W. B. Zimmerman and G. M. Homsy, Phys. Fluids A **3**, 1859 (1991).
[11] W. B. Zimmerman and G. M. Homsy, Phys. Fluids A **4**, 1901 (1992).
[12] W. B. Zimmerman and G. M. Homsy, Phys. Fluids A **4**, 2348 (1992).
[13] L. Gelhar, A. Gutjahr, and R. L. Naff, Water Resour. Res. **15**, 1387 (1979).
[14] L. W. Gelhar and C. L. Axness, Water Resour. Res. **19**, 161 (1983).
[15] G. Dagan, Annu. Rev. Fluid Mech. **19**, 183 (1987).
[16] A. De Wit, Phys. Fluids **7**, 2553 (1995).
[17] P. Indelman and B. Abramovich, Water Resour. Res. **30**, 1857 (1994).
[18] C.-T. Tan and G. M. Homsy, Phys. Fluids A **4**, 1099 (1992).
[19] H. A. Tchelepi, F. M. Orr, Jr., N. Rakotomalala, D. Salin, and R. Woemeni, Phys. Fluids A **5**, 1558 (1993).
[20] K. Sorbie, F. Feghi, G. E. Pickup, P. S. Ringrose, and J. L. Jensen, SPE/DOE Eighth Symposium on Enhanced Oil Recovery 1992 (unpublished), SPE/DOE 24140, p. 371.
[21] R. Lenormand, Transp. Porous Media **18**, 245 (1995).
[22] A. Zick and G. M. Homsy, J. Fluid Mech. **115**, 13 (1982).
[23] A. De Wit and G. M. Homsy, J. Chem. Phys. **107**, 9619 (1997), following paper.
[24] E. Meiburg and G. M. Homsy, *Numerical Simulation in Oil Recovery IMA 11* (Springer, Berlin, 1988), pp. 199–225.